

Observation of an Fe(II) Spin-Crossover in a Cesium Iron Hexacyanochromate

Wataru Kosaka,[†] Kiyoshi Nomura,[†] Kazuhito Hashimoto,^{*,†} and Shin-ichi Ohkoshi^{*,†,‡}

Department of Applied Chemistry, School of Engineering, The University of Tokyo, 7-3-1 Hongo, Bunkyo-ku, Tokyo 113-8656, Japan, and PRESTO, JST, 4-1-8 Honcho Kawaguchi, Saitama 332-0012, Japan

Received January 8, 2005; E-mail: hashimoto@light.t.u-tokyo.ac.jp; ohkoshi@light.t.u-tokyo.ac.jp

Thermal phase transition phenomenon, which is caused by spin-crossover, has been extensively investigated in solid-state chemistry. The spin-crossover phase transition has been observed in d^4 – d^7 octahedral coordination transition metal ions.^{1,2} In a spin-crossover complex, a transition metal ion can be in either the low-spin (ls) or the high-spin (hs) state depending on the strength of the ligand field. When the thermal energy is close to the exchange energy that corresponds to the crossover, a spin transition occurs between the two spin states. In the field of solid-state chemistry, studies on functionalized molecule-based magnets have also received much attention. Cyano-bridged metal assemblies³ are good systems for novel functional magnetic materials since they exhibit responses to external stimuli such as humidity⁴ and light.^{5,6} In this work, we observed a spin-crossover phenomenon in a cesium iron hexacyanochromate, which is a Prussian blue analogue. This compound exhibited a thermal phase transition with transition temperatures of 211 K ($T_{1/2l}$) and 238 K ($T_{1/2t}$) due to a spin-crossover on Fe^{II} sites. This spin-crossover phase transition is accompanied by a lattice contraction of 0.38 Å, but maintains a face-centered cubic (fcc) structure $F\bar{4}3m$. This is the first observation of Fe^{II} spin-crossover in a series of Prussian blue analogues.

The target compound was prepared by reacting a mixed aqueous solution of $K_3[Cr^{III}(CN)_6]$ (0.01 mol dm⁻³) and Cs^+Cl^- (1 mol dm⁻³) with a mixed aqueous solution of $Fe^{II}Cl_2$ (0.01 mol dm⁻³) and Cs^+I^- (1 mol dm⁻³). The obtained precipitate was a brown powder, and elemental analyses by inductively coupled plasma mass spectrometry and standard microanalytical methods showed that it had a composition of $CsFeCr(CN)_6 \cdot 1.3H_2O$. Calcd: Cs, 31.6; Fe, 13.3; Cr, 12.4; C, 17.1; H, 0.6; N, 20.0. Found: Cs, 31.5; Fe, 13.3; Cr, 12.4; C, 17.3; H, 0.6; N, 19.9. Scanning electron microscope (SEM) images showed that the prepared sample consists of cubic microcrystals of ca. 200 nm (Supporting Information).

Magnetic measurements were conducted using a superconducting quantum interference device (SQUID) magnetometer (Quantum Design MPMS-5). Figure 1 shows the temperature dependence of the product of the molar magnetic susceptibility (χ_M) and the temperature (T) at a rate of 1 K min⁻¹ in an external magnetic field of 5000 G. The $\chi_M T$ value was 6.11 K cm³ mol⁻¹ (high-temperature (HT) phase) at 280 K. As the temperature decreased, the $\chi_M T$ value sharply decreased around 210 K and reached a local minimum of 2.66 K cm³ mol⁻¹ at 188 K (low-temperature (LT) phase). Conversely, as the sample in the LT phase was warmed, the $\chi_M T$ value increased around 230 K and returned to the HT phase value at 250 K. The transition temperatures of HT \rightarrow LT ($T_{1/2l}$) and LT \rightarrow HT ($T_{1/2t}$) were 211 and 238 K, respectively, and the width of the thermal hysteresis loop ($\Delta T = T_{1/2t} - T_{1/2l}$) was 27 K. This thermal phase transition was repeatedly observed several times.

Figure 2 shows the temperature dependence of the CN⁻ stretching frequencies in the IR spectra. In the HT phase at 280 K, a strong

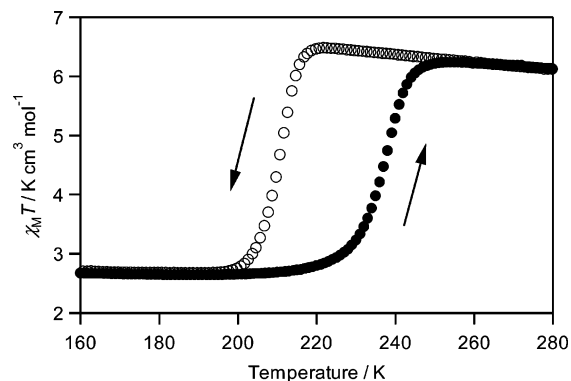


Figure 1. Temperature dependence of $\chi_M T - T$ plots of cesium iron hexacyanochromate in an external magnetic field of 5000 G; measured while cooling (○) and warming (●).

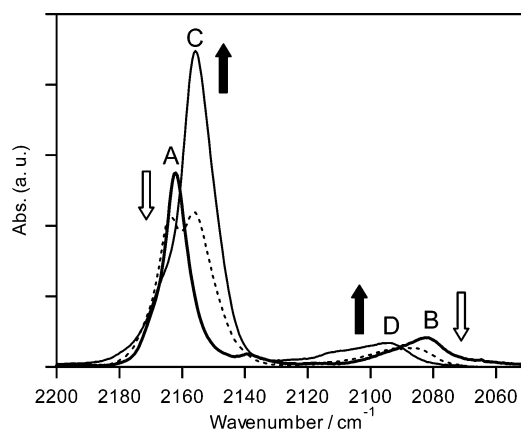


Figure 2. Temperature dependence of the CN⁻ stretching frequencies in the IR spectra as the temperature decreases; measured at 280 K (bold line), 205 K (dotted line), and 180 K (fine line).

peak at 2163 cm⁻¹ (A) and a weak peak at 2083 cm⁻¹ (B) were observed. Peaks A and B are assigned to Cr^{III}–CN–Fe^{II}_{hs} and Cr^{III}–NC–Fe^{II}_{ls} of the cyano flip,⁷ respectively. As the temperature decreased, these two peaks decreased, and two new peaks appeared at 2156 cm⁻¹ (C) and 2095 cm⁻¹ (D) around $T_{1/2l}$. Peak C is assigned to Cr^{III}–CN–Fe^{II}_{ls}, which is converted from peak A. Peak D is Cr^{III}–NC–Fe^{II}_{ls}, which is from a shift in peak B due to the variation in the cyano group between the HT and LT phases. The IR spectra indicate that the electronic states of HT and LT phases are $Cs^I\{Fe^{II}_{hs}[Cr^{III}(CN)_6]\}_{0.94}\{Fe^{II}_{ls}[Cr^{III}(NC)_6]\}_{0.06} \cdot 1.3H_2O$ and $Cs^I\{Fe^{II}_{hs0.12}Fe^{II}_{ls0.88}[Cr^{III}(CN)_6]\}_{0.94}\{Fe^{II}_{ls}[Cr^{III}(NC)_6]\}_{0.06} \cdot 1.3H_2O$, respectively.⁸ In the HT phase, 94% of Fe^{II} is in the hs state and 6% is the ls state. In contrast, 11% ($= (0.12 \times 0.94) \times 100$) of Fe^{II} is the hs state and 89% ($= (0.88 \times 0.94 + 0.06) \times 100$) of Fe^{II} is the ls state in the LT phase.

The Fe^{II} spin-crossover was also confirmed by ⁵⁷Fe Mössbauer spectroscopy (Supporting Information). In the HT phase, a doublet

[†] The University of Tokyo.

[‡] PRESTO, JST.

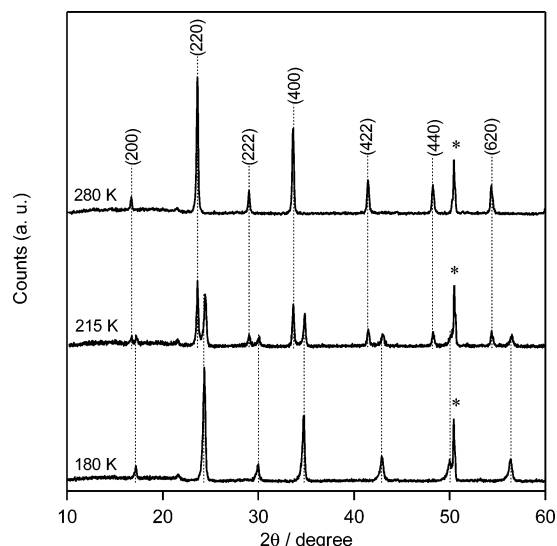


Figure 3. Temperature dependences of XRD spectra for cesium iron hexacyanochromate as the temperature decreases. (* indicates Cu from the sample holder).

peak was mainly observed (isomer shift = 1.07; quadrupole splitting = 0.74), which is assigned to $\text{Fe}^{\text{II}}_{\text{hs}}$. In the LT phase, this doublet peak disappeared and a singlet peak appeared (isomer shift = 0.44), which is assigned to $\text{Fe}^{\text{II}}_{\text{ls}}$. These results show that the spin-crossover actually occurred on Fe^{II} sites.

The temperature dependence of the X-ray powder diffraction (XRD) patterns showed that the present spin-crossover is accompanied by a structural phase transition (Figure 3). The XRD patterns of the HT phase at 280 K showed an fcc $F\bar{4}3m$ structure with a lattice constant of 10.708(1) Å. In contrast, the LT phase showed XRD patterns of an fcc $F\bar{4}3m$ structure with a lattice constant of 10.330(1) Å. The lattice constant in the LT phase decreased by about 0.38 Å compared to that in the HT phase. This structural phase transition was repeatedly observed.

The CsFeCr Prussian blue analogue clearly showed a spin-crossover transition, but in the analogue compound of $\text{Fe}[\text{Cr}(\text{CN})_6]_{2/3} \cdot 5\text{H}_2\text{O}$ a spin-crossover was not observed.⁵ In this analogue compound, typically Fe^{II} is coordinated by four N atoms from cyano groups and two O atoms from ligand waters and the statistical probabilities of each coordinate geometry are 8.8% ($\text{Fe}^{\text{II}}\text{N}_6$), 26.4% ($\text{Fe}^{\text{II}}\text{N}_5\text{O}$), 33.0% ($\text{Fe}^{\text{II}}\text{N}_4\text{O}_2$), 22.0% ($\text{Fe}^{\text{II}}\text{N}_3\text{O}_3$), 8.2% ($\text{Fe}^{\text{II}}\text{N}_2\text{O}_4$), and 1.6% ($\text{Fe}^{\text{II}}\text{NO}_5$) (Supporting Information). For the spin-crossover phenomenon to appear, the number of cyanonitrogen around Fe^{II} must be significant. Maybe in $\text{Fe}[\text{Cr}(\text{CN})_6]_{2/3} \cdot 5\text{H}_2\text{O}$ the strength of the ligand field is insufficient to cause the spin-crossover. In contrast, $\text{Fe}^{\text{II}}\text{N}_6$ in the CsFeCr Prussian blue analogue is an environmental advantage for the spin-crossover. Furthermore, since both Fe^{II} and Cr^{III} are bridged by a CN^- group with six-coordinate, the interaction between spin-crossover sites should be stronger in the 3D structure.

The field-cooled magnetization curve at an external magnetic field of 10 G revealed that the LT phase had a spontaneous magnetization with a magnetic ordering temperature of 9 K and the saturation magnetization (M_S) at 2 K was $3.3 \mu_B$ (Supporting Information). The observed M_S value of $3.3 \mu_B$ is consistent with the expected M_S value of $3.4 \mu_B$ due to the sum of sublattice magnetization of Cr^{III} and the remaining $\text{Fe}^{\text{II}}_{\text{hs}}$ for a given formula of the LT phase.

In summary, we found that a cesium iron hexacyanochromate showed a spin-crossover behavior. The spin-crossover phenomenon in a Prussian blue analogue allows a variety of new functionalities to be considered. For example, the observation of photoinduced magnetization caused by a light-induced excited spin state trapping effect⁹ is expected since this material has a spontaneous magnetization.

Acknowledgment. We thank Dr. H. Tokoro, Mr. T. Matsuda, and Mr. K. Kida for helpful discussions. The present research is supported in part by a Grant for 21st Century COE Program “Human-Friendly Materials based on Chemistry” and a Grand-in-Aid for Scientific Research from the Ministry of Education, Culture, Sports, Science, and Technology of Japan.

Supporting Information Available: SEM image of the precipitate, ^{57}Fe Mössbauer spectra of HT and LT phases, statistical probabilities of coordinate geometries around Fe in $\text{Fe}[\text{Cr}(\text{CN})_6]_{2/3} \cdot 5\text{H}_2\text{O}$, analysis of $\chi_M T - T$ curves, magnetization versus temperature plots, and magnetization versus external magnetic field plots of the LT phase. This material is available free of charge via the Internet at <http://pubs.acs.org>.

References

- (1) (a) Kahn, O. *Molecular Magnetism*; VCH: New York, 1993. (b) König, E. *Prog. Inorg. Chem.* **1987**, 35, 527. (c) Kahn, O.; Kröber, J.; Jay, C. *Adv. Mater.* **1992**, 4, 718. (d) Gülich, P.; Hauser, A.; Spiering, H. *Angew. Chem., Int. Ed. Engl.* **1994**, 33, 2024. (e) Gülich, P.; Garcia, Y.; Goodwin, H. A. *Chem. Soc. Rev.* **2000**, 29, 419. (f) Real, J. A.; Gaspar, A. B.; Niel, V.; Muñoz, M. C. *Coord. Chem. Rev.* **2003**, 236, 121.
- (2) (a) Real, J. A.; Andrés, E.; Muñoz, M. C.; Julve, M.; Granier, T.; Bousseksou, A.; Varret, F. *Science* **1995**, 268, 265. (b) Létard, J. F.; Guionneau, P.; Codjovi, E.; Lavastre, O.; Bravic, G.; Chasseau, D.; Kahn, O. *J. Am. Chem. Soc.* **1997**, 119, 10861. (c) Boukheddaden, K.; Shteto, I.; Hôo, B.; Varret, F. *Phys. Rev. B* **2000**, 62, 14796. (d) Herchel, R.; Boča, R.; Gembický, M.; Kozisek, J.; Renz, F. *Inorg. Chem.* **2004**, 43, 4103.
- (3) (a) Ferlay, S.; Mallah, T.; Ouahès, R.; Veillet, P.; Verdaguer, M. *Nature* **1995**, 378, 701. (b) Buschmann, W. E.; Paulson, S. C.; Wynn, C. M.; Girtu, M. A.; Epstein, A. J.; White, H. S.; Miller, J. S. *Adv. Mater.* **1997**, 9, 645. (c) Holmes, S. M.; Girolami, G. S. *J. Am. Chem. Soc.* **1999**, 121, 5593. (d) Hatlevik, Ø.; Buschmann, W. E.; Zhang, J.; Manson, J. L.; Miller, J. S. *Adv. Mater.* **1999**, 11, 914. (e) Ohkoshi, S.; Mizuno, M.; Hung, G. J.; Hashimoto, K. *J. Phys. Chem. B* **2000**, 104, 9365.
- (4) Ohkoshi, S.; Arai, K.; Sato, Y.; Hashimoto, K. *Nat. Mater.* **2004**, 3, 857.
- (5) (a) Ohkoshi, S.; Yoroze, S.; Sato, O.; Iyoda, T.; Fujishima, A.; Hashimoto, K. *Appl. Phys. Lett.* **1997**, 70, 1040. (b) Ohkoshi, S.; Einaga, Y.; Fujishima, A.; Hashimoto, K. *J. Electroanal. Chem.* **1999**, 473, 245. (c) Ohkoshi, S.; Hashimoto, K. *J. Am. Chem. Soc.* **1999**, 121, 10591.
- (6) (a) Sato, O.; Iyoda, T.; Fujishima, A.; Hashimoto, K. *Science* **1996**, 272, 704. (b) Bleuzen, A.; Lomenech, C.; Escax, V.; Villain, F.; Varret, F.; Cartier dit Moulin, C.; Verdaguer, M. *J. Am. Chem. Soc.* **2000**, 122, 6648. (c) Pejakov, D. A.; Manson, J. L.; Miller, J. S.; Epstein, A. J. *Phys. Rev. Lett.* **2000**, 85, 1994. (d) Ohkoshi, S.; Machida, N.; Zhong, Z. J.; Hashimoto, K. *Synth. Met.* **2001**, 122, 523. (e) Rombaut, G.; Verelst, M.; Golhen, S.; Ouahab, L.; Mathonière, C.; Kahn, O. *Inorg. Chem.* **2001**, 40, 1151. (f) Tokoro, H.; Ohkoshi, S.; Hashimoto, K. *Appl. Phys. Lett.* **2003**, 82, 1245. (g) Arimoto, Y.; Ohkoshi, S.; Zhong, Z. J.; Seino, H.; Mizobe, Y.; Hashimoto, K. *J. Am. Chem. Soc.* **2003**, 125, 9240. (h) Herrera, J. M.; Marvaud, V.; Verdaguer, M.; Marrot, J.; Kalisz, M.; Mathonière, C. *Angew. Chem., Int. Ed.* **2004**, 43, 2.
- (7) (a) Shriver, D. F.; Shriver, S. A.; Anderson, S. E. *Inorg. Chem.* **1965**, 4, 725. (b) Brown, D. B.; Shriver, D. F.; Schwartz, L. H. *Inorg. Chem.* **1968**, 7, 77.
- (8) The estimated oscillator strength ratio of peak A ($\text{Cr}^{\text{III}}\text{—CN—Fe}^{\text{II}}_{\text{hs}}$) to peak C ($\text{Cr}^{\text{III}}\text{—CN—Fe}^{\text{II}}_{\text{ls}}$) in the IR spectra was 1.8. A compound that contains more cyano flips can be obtained by heating. In this heated sample, peak A was converted to peak B ($\text{Cr}^{\text{III}}\text{—NC—Fe}^{\text{II}}_{\text{ls}}$). Comparing the IR spectra of the heated sample and the original sample, we estimated that the oscillator strength ratio of peak A to peak B was 2.1.
- (9) (a) Decurtins, S.; Gülich, P.; Köhler, C. P.; Spiering, H.; Hauser, A. *Chem. Phys. Lett.* **1984**, 105, 1. (b) Decurtins, S.; Gülich, P.; Hasselbach, K. M.; Spiering, H.; Hauser, A. *Inorg. Chem.* **1985**, 24, 2174. (c) Létard, J. F.; Real, J. A.; Moliner, N.; Gaspar, A. B.; Capes, L.; Cador, O.; Kahn, O. *J. Am. Chem. Soc.* **1999**, 121, 10630.

JA050118L

Observation of an Fe(II) Spin-Crossover in a Cesium Iron Hexacyanochromate

Wataru Kosaka,[†] Kiyoshi Nomura,[†] Kazuhito Hashimoto,^{*,†} and Shin-ichi Ohkoshi^{*,†,‡}

[†] *Department of Applied Chemistry, School of Engineering, The University of Tokyo,
7-3-1 Hongo, Bunkyo-ku, Tokyo 113-8656, Japan*

[‡] *PRESTO, JST, 4-1-8 Honcho Kawaguchi, Saitama 332-0012, Japan*

e-mail: ohkoshi@light.t.u-tokyo.ac.jp

SUPPORTING INFORMATION

SEM image:

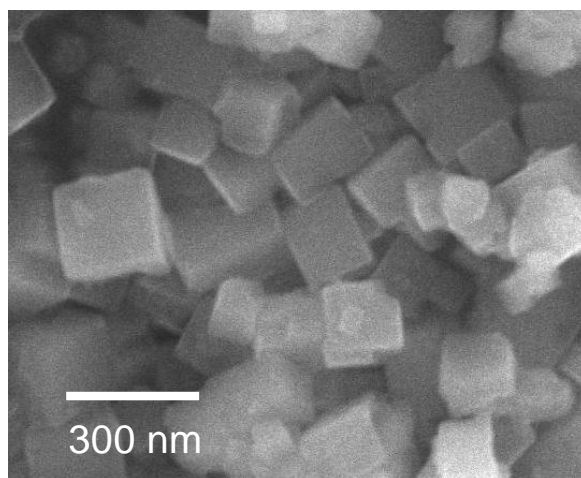


Figure S1. SEM image of the CsFeCr(CN)₆·1.3H₂O

⁵⁷Fe Mössbauer spectra of HT and LT phases:

At 235 K, a doublet peak (I) was mainly observed (85%), which is assigned to $\text{Fe}^{\text{II}}_{hs}$. At 170 K, this doublet peak disappeared and a singlet peak (II) appeared, which is assigned to $\text{Fe}^{\text{II}}_{ls}$. These results show that the spin crossover actually occurred on Fe^{II} sites. A small doublet peak (III) and a singlet peak (IV) were observed at both temperatures. The peak (III) is assigned to the remaining $\text{Fe}^{\text{II}}_{hs}$ in LT phase, and the peak (IV) is assigned to $\text{Fe}^{\text{II}}_{ls}$ of cyano flip.

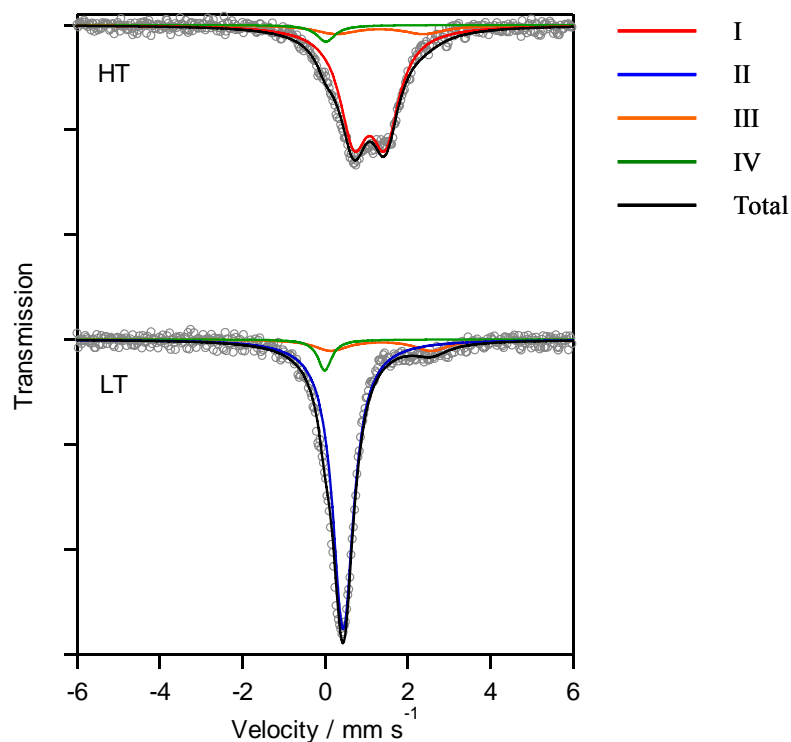


Figure S2. ⁵⁷Fe Mössbauer spectra of HT phase (235 K) and LT phase (170 K) in the cooling process.

Table S1. ⁵⁷Fe Mössbauer parameters of HT phase and LT phase.

	HT phase (235 K)			LT phase (170 K)			assignment
	area	IS	QS	area	IS	QS	
I	85%	1.07	0.74	—	—	—	$\text{Fe}^{\text{II}}_{hs} - \text{NC}$
II	—	—	—	84%	0.44	0	$\text{Fe}^{\text{II}}_{ls} - \text{NC}$
III	10%	1.32	2.12	10%	1.36	2.43	$\text{Fe}^{\text{II}}_{hs} - \text{NC}$
IV	5%	0.02	0	6%	-0.01	0	$\text{Fe}^{\text{II}}_{ls} - \text{CN}$

Statistical probabilities of coordinate geometries around Fe in $\text{Fe}[\text{Cr}(\text{CN})_6]_{2/3} \cdot 5\text{H}_2\text{O}$:

In $\text{Fe}^{\text{II}}[\text{Cr}^{\text{III}}(\text{CN})_6]_{2/3} \cdot 5\text{H}_2\text{O}$, vacancies randomly exist in the lattice as shown in Figure S3. The statistical probabilities of $\text{Fe}^{\text{II}}\text{N}_6$, $\text{Fe}^{\text{II}}\text{N}_5\text{O}$, $\text{Fe}^{\text{II}}\text{N}_4\text{O}_2$, $\text{Fe}^{\text{II}}\text{N}_3\text{O}_3$, $\text{Fe}^{\text{II}}\text{N}_2\text{O}_4$, and $\text{Fe}^{\text{II}}\text{NO}_5$ are expressed by the product of the combination (${}_6\text{C}_n$; $n = 0 - 5$) and existing probabilities of $1/3$ and $2/3$ for O and N atoms, that is, ${}_6\text{C}_n(1/3)^n(2/3)^{6-n}$, where n is the number of O atoms.

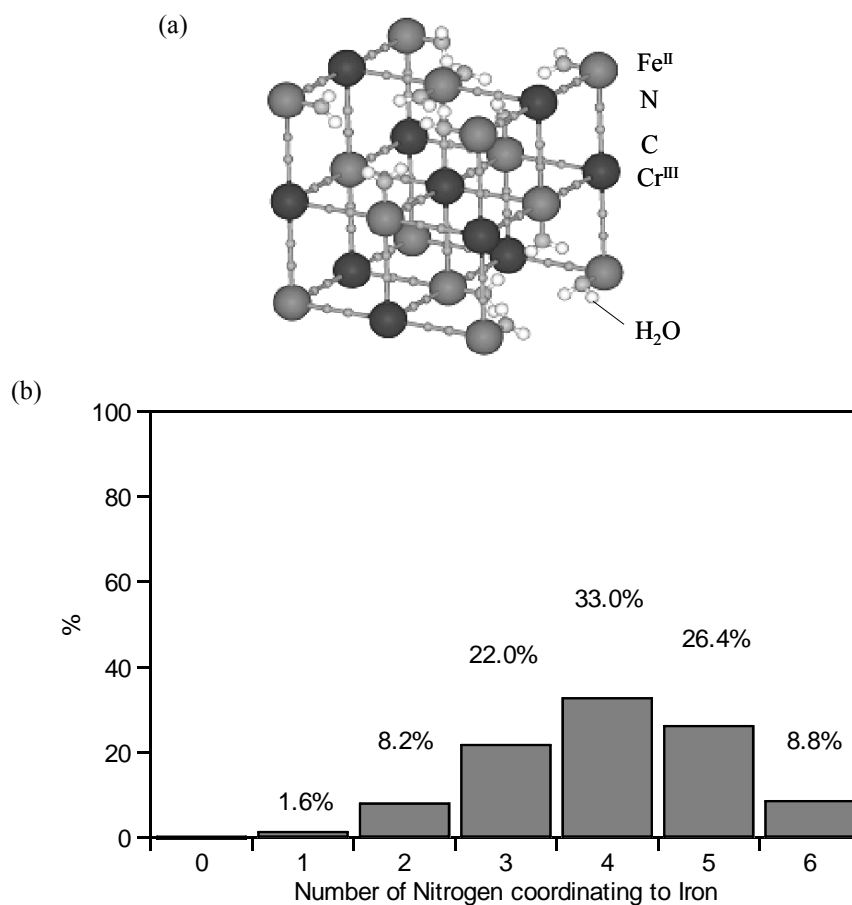


Figure S3. (a) Schematic illustration of the crystal structure of $\text{Fe}^{\text{II}}[\text{Cr}^{\text{III}}(\text{CN})_6]_{2/3} \cdot 5\text{H}_2\text{O}$. Ligand water molecules coordinate to Fe^{II} around the vacancies of $[\text{Cr}^{\text{III}}(\text{CN})_6]$. Zeolitic water molecules are here omitted. (b) The statistical probabilities of possible coordinating geometries around Fe^{II} .

Analysis of $\chi_M T$ - T curves:

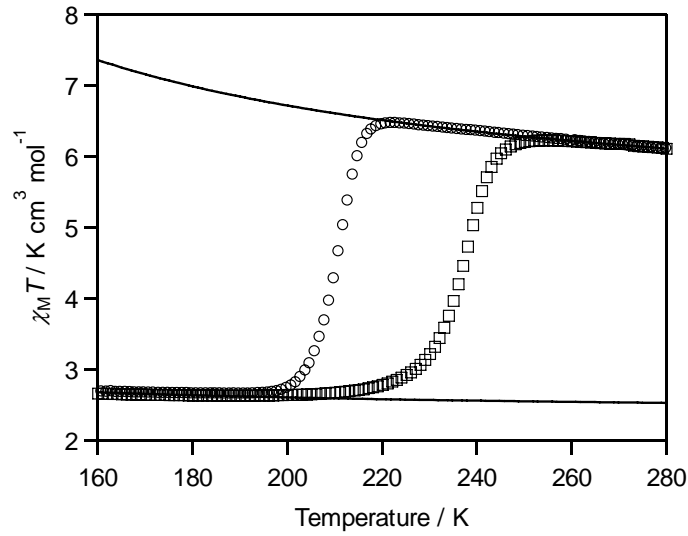


Figure S4. The analysis of the $\chi_M T$ - T curves of HT and LT phases using a molecular field theory, i.e., HT phase ($\text{Fe}^{\text{II}}_{hs}$: $S = 2$, Cr^{III} : $S = 3/2$) with $J_{\text{FeCr}} = +1.9 \text{ cm}^{-1}$, $g_{\text{Fe}} = 2.1$, and $g_{\text{Cr}} = 2.0$, and LT phase (89% $\text{Fe}^{\text{II}}_{ls}$: $S = 0$, 11% $\text{Fe}^{\text{II}}_{hs}$: $S = 2$; Cr^{III} : $S = 3/2$) with $J_{\text{CrCr}} = +1.1 \text{ cm}^{-1}$, $g_{\text{Fe}} = 2.1$, and $g_{\text{Cr}} = 2.0$.

Magnetic property of LT phase:

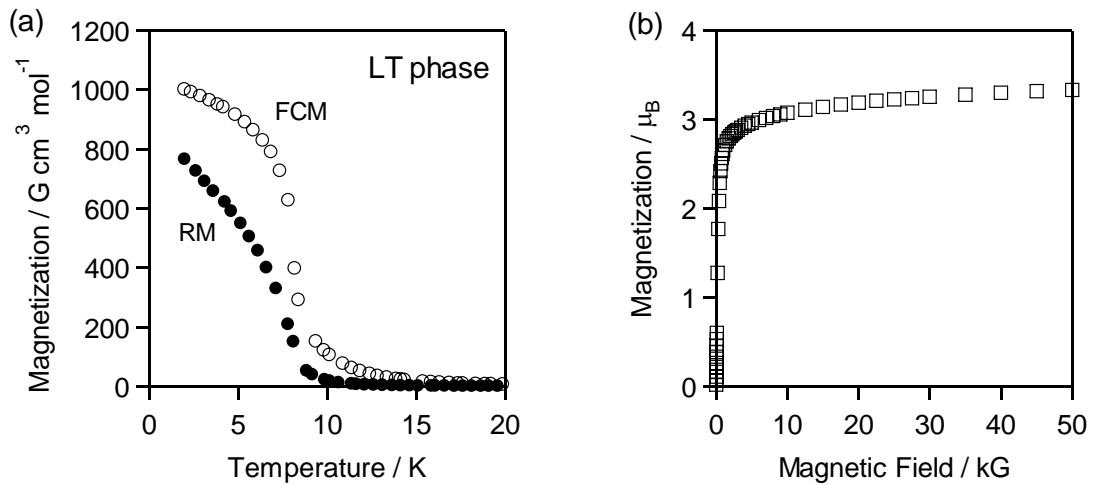


Figure S5. (a) Field-cooled magnetization (FCM) and remnant magnetization (RM) curves of the LT phase in an external magnetic field of 10 G. (b) Magnetization vs. external magnetic field plots of the LT phase at 2K.